# 3D Plant Modelling via Hyperspectral Imaging

Jie Liang
Australian National University
Australia
jie.liang@anu.edu.au

Ali Zia
Griffith University
Australia
ali.zia@griffithuni.edu.au

Jun Zhou
Griffith University
Australia
jun.zhou@griffith.edu.au

Xavier Sirault
CSIRO
Australia
xavier.sirault@csiro.au

## Abstract

*Plant phenomics research requires different types of sensors be employed to measure the physical traits of plant surface and to estimate the plant biomass. Of particular interest is the hyperspectral imaging device which captures wavelength indexed band images that characterise material properties of objects under study. In this paper, we introduce a proof of concept research that builds 3D plant model directly from hyperspectral images captured in a controlled lab environment. We show that hyperspectral imaging has shown clear advantages in segmenting plant from its background and is promising in generating comprehensive 3D plant models.*

## 1. Introduction

Plant phenomics is an area of plant biology that studies the influence of genetics and environment on both the physical and biochemical traits of plant organisms [7]. One of the main tasks in this area is dissecting plant function and performance via measurement of plant appearance. Such measurements provide inputs to other key tasks in plant phenomics, including investigating carbon partitioning and photosynthesis in plants, as well as finding mechanisms of drought tolerance and flowering behavior. Therefore, robust and accurate plant measurement methods are of great importance.

The development of sensing technology has enabled many measurement tools such as radar, RGB camera, infrared camera and hyperspectral camera be bedded in plant observation process. Among them, of particular interest is the hyperspectral imaging device, which generates tens or hundreds of contiguous narrow spectral band images indexed by the light wavelength. These band images contain rich information on the spectral and spatial distributions of distinct surface materials. They enable more accurate and reliable object detection and material classification than using panchromatic or multispectral imagery. As a consequence, hyperspectral imaging techniques have been widely used in remote sensing, environmental monitoring, and surveillance in agriculture, industry and military [9]. When applied to plant research, hyperspectral imaging has shown success in detecting traits of disease or nutrition deficient [6, 1].

Despite its advantages in object detection and analysis, the research on hyperspectral imaging in computer vision is still very limited. In recent years, thanks to the production of relatively low cost hyperspectral imaging devices, computer vision researchers have started to explore this area. More understanding of the statistical properties of hyperspectral imagery have been reached [4], and some traditional computer vision topics have been covered, such as camera sensitivity analysis [10], feature extraction [13], and illumination estimation [8].

In this paper, we address one of the fundamental problems of computer vision, 3D reconstruction, in the context of plant modelling using hyperspectral images. Some research have already incorporated hyperspectral data into 3D models. For example, Brusco et al presented an interesting work on modeling historical building with multispectral data, while the depth information was captured by a range camera based on laser scanner [2]. Similarly, Nieto et al built 3D model based on depth data captured by a laser scanner and mapped hyperspectral image to 3D Model to display geological mineral information [16]. More recently, Kim et al integrated a hyperspectral camera into a 3D scanning system to enable the measurement of the diffuse spectral reflectance and fluorescence of specimens [12]. However, all of these have not explicitly built 3D models directly from hyperspectral data.

Our method, on the contrary, attempts to build a 3D plant model directly from a sequence of hyperspectral images captured in a controlled lab environment. The spectral data is first used to segment plant from its background. Then keypoints are extracted from plant, which are used to find correspondences between a pair of spectral images. Finally a structure from motion based model is developed to reconstruct the 3D plant. The initial results show that the spectral data can be used for effective plant segmentation, which is an important step for 3D modelling. Furthermore, the 3D models produced from difference bands contains mostly consistent structural information of plants, and in some cases, complement each other. This implies that different band images can capture different properties of plant surface. If these models can be properly combined, they will lead to promising approach in building a 3D model that reflects more complete structural information of the plants than that can be reconstructed by traditional systems [17, 20]. This technique can also be combined with existing 3D plant modelling methods based on laser scanners or Kinect [15] in order to build more accurate plant models.

The rest of paper is organised as follows. Section 2 describes the hyperspectral plant imaging system. Section 3 introduces the proposed 3D plant modelling method. Section 4 presents the experimental results, with conclusions and future work given in Section 5.

## 2. Hyperspectral Imaging of Plants

Our hyperspectral imaging system consists of three main components, i.e. objective lens, a hyperspectral filter, and a high sensitivity camera, with the hyperspectral filter connecting the lens and the camera. In this research, we have used an acousto-optical tunable filter (AOTF) that supports imaging from 400nm to 1000nm at 10nm in spectral resolution. A control unit is connected to the filter to let the light in designated wavelength pass through to reach the camera. By scanning through the visible to infrared wavelength, grayscale images can be generated to form different bands of the hyperspectral image. The output of the imaging process is a data cube with the first two dimensions show the spatial positions of pixels, and the third dimension indexes the bands. Therefore, each pixel on the image is a vector of responses across the visible to infrared spectrum.

We collected plant data in the High Resolution Plant Phenomics Centre (HRPPC) in the Commonwealth Scientific and Industrial Research Organisation (CSIRO) in Canberra, Australia. HRPPC provides integrated plant measurement system that utilises several imaging tools, such as light detection and ranging sensors, thermal infrared cameras, multispectral and RGB cameras to capture high resolution plant data. The imaging lab provides consistent illumination condition to facilitate the imaging process. During the data capture, a plant was put on a turntable platform and transmitted into the workspace. After the plant was positioned, the hyperspectral camera captured images by scanning through the visible to infrared bands. Then the platform rotated for three degrees to allow another scan being done. This process continued until the plant had been rotated for 360 degrees with all views covered. During the imaging process, camera parameters such as focus length, zoom, exposure time remained unchanged. At last, 120 data cubes were obtained for each plant, covering the whole surface of the plant. During the image capture process, a white balance reflectance target is used to normalised the hyperspectral data. Figure 1 shows a plant image example. The first row of the figure shows band images captured at different wavelength from the same angle, while the second row shows images captured at different angles from the same band.

## 3. Plant 3D Modeling

The proposed 3D modelling method contains three steps, which are image quality improvement, plant segmentation, and 3D reconstructing. The first two steps can be considered as the preprocessing steps.

### 3.1. Image Preprocessing

The hyperspectral images often suffer from noise and cross band misalignment. The noises mainly come from the narrow band of light that is allowed to pass the hyperspectral filter within short period of time. Although our camera is highly sensitive, the signal to noise ratio is still low, especially in the short wavelength range where the light intensity is low. To reduce the influence of these bands, those with very low signal to noise ratio were removed from the data. Then the rest band images were smoothed using a Gaussian filter.

Misalignment of band image can be caused by the chromatic abberation of camera lens, or the misalignment of grating component in the tunable filter. Then light in different wavelength follows slightly different transmission paths before reaching the camera. In order to reduce the misalignment, each band image is calibrated against an anchor band image at 790nm. This is done by maximising the mutual information of every band to the anchor band, so that the transformation matrix in the following equation can be optimised:

$$\begin{bmatrix} x' \\ y' \\ 1 \end{bmatrix} = \begin{bmatrix} s\cos(\theta) & -s\sin(\theta) & t_x \\ s\sin(\theta) & s\cos(\theta) & t_y \\ 0 & 0 & 1 \end{bmatrix} \begin{bmatrix} x \\ y \\ 1 \end{bmatrix} \tag{1}$$

In this equation, $\begin{bmatrix} x' & y' & 1 \end{bmatrix}^T$ and $\begin{bmatrix} x & y & 1 \end{bmatrix}^T$ are pixels before and after transformation, respectively. $\theta$, $s$, $t_x$, and

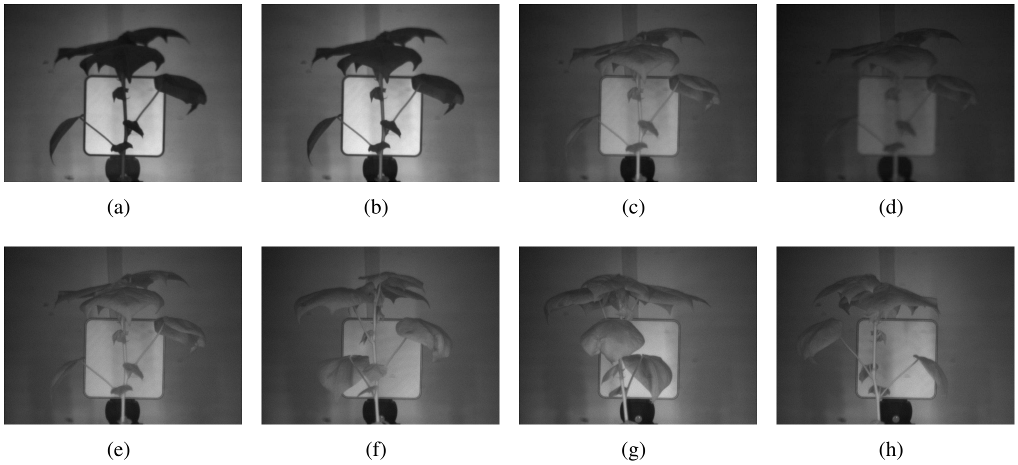


Figure 1. Hyperspectral images: the first row shows band images captured at 600nm, 700nm, 800nm and 900nm from 0 degree; the second row shows band images captured at 800nm from 0 degree, 60 degrees, 120 degrees, and 180 degrees, respectively.

$t_y$ are in-plane rotation angle, scale, and translation parameters. After the transformation matrices had been obtained for each band, a linear regression fitting is performed on the transformation matrices, so as to make the changes smooth across different bands.

After quality improvement operations, the next step is to segment plant image from its background. In this task, hyperspectral data provides much more information on the plant material property of objects than that can be captured from RGB or monochrome images. It shows fine spectral reflectance changes of the plant surface, which is very useful for segmenting plant from its environment. Another spectral property that is very useful for the plant segmentation is that in the near infrared wavelength, plants look much brighter than they appear in the visible range because of the low absorption rate of plant in the range. The hyperspectral data can clearly capture such property, as shown in the last two images of the first row in Figure 1.

To segment plants from their background, we have explored two classification methods, including K-means clustering and support vector machines. The principle of K-means clustering is to minimize the within cluster sum square error of the whole image, which does not require training data. SVM classifier, on the other hand, tries to find an optimal hyperplane to distinguish plant pixels from neighboring background pixels. Details on how these two methods were implemented are described in Section 4.

### 3.2. 3D modeling

Once a plant is segmented from its background, 3D models are built from the hyperspectral band image sequence captured at different angles. Here, we followed a band-by-band 3D modelling strategy, i.e., one 3D model is built from each band. At each band, our approach follows the standard structure from motion method as introduced in [11]. This approach consists of four key steps. They are feature extraction, feature matching, geometry estimation, and 3D project of key points.

In the feature extraction step, SIFT keypoints are detected with descriptor generated [14]. Then the features in different angle images are matched using the histogram-based descriptors to get the correspondences for combination of images. Because there are 120 images captured from different angles, there would be 7140 pairwise matches.

In terms of 3D reconstruction, suppose the set of image correspondences are $\mathbf{x}_i \leftrightarrow \mathbf{x}'_i$ and assume that these correspondences comes from a set of 3D points $\mathbf{X}_i$ , which are unknown. Similarly, the position, orientation and calibration of the cameras are not known. The reconstruction task is to find the camera matrices $P$ and $P'$, as well as the 3D points $\mathbf{X}_i$ such that each pair of points satisfies

$$\mathbf{x}_i = P\mathbf{X}_i, \tag{2}$$

and

$$\mathbf{x}'_i = P'\mathbf{X}_i, \tag{3}$$

There are two steps in the geometry estimation phase. First, fundamental matrix is computed from point correspondences and then the camera matrices are computed from fundamental matrix. To compute fundamental matrix $F$, suppose we have $\mathbf{x}_i \leftrightarrow \mathbf{x}'_i$ correspondences of two images, the fundamental matrix satisfies the condition $\mathbf{x}'_i F \mathbf{x}_i = 0$ for all $i$. With the $\mathbf{x}_i$ and $\mathbf{x}'_i$ known, this equation is linear in the (unknown) entries of the matrix $F$. Given at least 8 point correspondences, entries of $F$ can be solved linearly. With more than 8 equations, a least-squares solution is can be adopted. If $P$ and $P'$ are pair of camera matrices corresponding to fundamental matrix $F$, then they are computes as follows

$$P = [I|0] \tag{4}$$

and

$$P' = [[e'] \times F|e'] \tag{5}$$

where $e'$ is the epipole such that $e'TF = 0$ [11].

The 3D projection of keypoint consists of a process known as triangulation. Let $P$ and $P'$ be camera matrices and $\mathbf{x}$ and $\mathbf{x}'$ be two points in two images that satisfy epipolar constraint $\mathbf{x}'TF\mathbf{x} = 0$. This constraint may be interpreted geometrically in terms of rays in space corresponding to two image points meaning that $x'$ lies on epipolar line $F\mathbf{X}$. So it means that two rays back-projected from image points $x$ and $x'$ lie in a common epipolar plane (plane passing through two camera centers). Since two ray lies in a plane they will intersect at some point. This point is $\mathbf{X}$ (3-D point) which is project via two camera point $\mathbf{x}$ and $\mathbf{x}'$ in two images [11].

During the 3D model reconstruction process, SIFT features and matches across image sequence are required so that correspondences among images can be determined. But unfortunately, due to the narrow bandwidth of the light allowed to reach the camera during the imaging process, hyperspectral images are often very noisy. This has greatly degraded the extracted features. Furthermore, the homogeneous nature of the plant leaves and stems makes it difficult to detect many SIFT keypoints from images. Therefore, the number of features obtained from each band are not sufficient to generate continuous correspondences between band images captured at neighboring angles. This leads to more than one disassociated 3D models be generated. To solve the insufficient feature problem, Canny edge detection [3] is employed to generate edges, and then SIFT keypoints are extracted at each edge point in order to generate more candidate keypoints for correspondence detection.

## 4. Experimental Results

We have carried out experiments on the acquired hyperspectral plant data. Each original data cube consists of 61 bands from 400nm to 1000nm with 10nm interval captured at 120 different angles. Band images in the 400nm to 590nm range were removed because of very low image quality, such that only 41 bands were used for the modelling, which correspond to 2GB data for each plant.

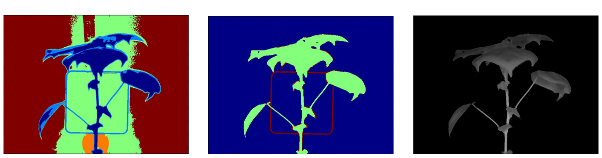

(a) (b) (c)

Figure 2. Segmentation results from a) K-means; b) SVM. c) shows the final segmented plant.

For the segmentation step, when K-means clustering were used, the scene was clustered into 4 classes: background, plant, calibration board, and base. The clustering method was initialised randomly, and iterated until convergence. When SVM was used, the classifier was trained on one manually labeled hyperspectral image, and then was used to classify all other images. To do so, we adopted the LIBSVM [5] toolbox. An RBF kernel was used with the default parameters for the SVM. Example results are shown in Figure 2, which tells that the SVM can generate better segmentation performance than the clustering method. In the feature extraction step, we extracted SIFT descriptors at edge points of plants. Examples of matched keypoints on images from two angles are given in 3. To generate the 3D model, we adopted virtual-SFM tool [18, 19].

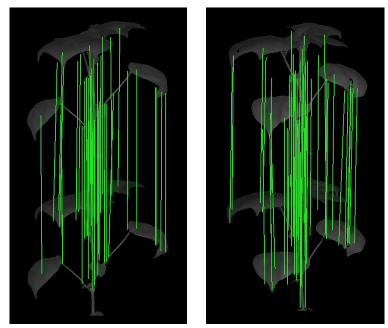

(a) (b)

Figure 3. Examples of matched keypoints.

Finally, some 3D reconstruction results are displayed in Figure 4. Images in the same row show 3D model observed from different viewing angles when constructed from the same band. From top to bottom, different rows of images show 3D models reconstructed at 600mn, 800mn, 850mn, and 900mn, respectively. 3D models at 700mn and 750nm can not be reconstructed because the reflectance of plant at these wavelengths is very low.

From the figure, it can be seen that the 3D models obtained are not perfect at this stage. From the 120 images, several models were generated. However each model only reconstructed parts of the plant, while the points cloud was not very accurate. This is mainly due to the low quality of the hyperspectral images, which makes it difficult to find sufficient features in the plant surface for correspondence calculation. This problem can be solved by increase the exposure so as to generate images with higher signal-to-noise ratio. On the other hand, it can be seen that different bands have generated different partial 3D models of the plant. These models compensate to each other, so that we can theoretically build a complete model by merging those partial models.

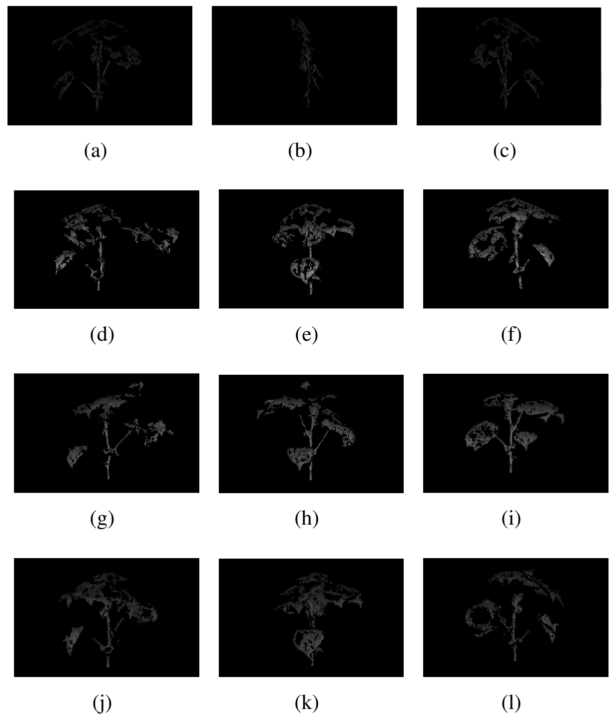


Figure 4. Different views of the 3D models at different wavelengths.

## 5. Conclusions

The proposed work is the first attempt to build a 3D hyperspectral plant model solely from hyperspectral images. The results show that the spectral information is beneficial to the plant segmentation, and that 3D models reconstructed from different wavelength bands are complement to each other. This work opens new dimensions that can be explored in 3D modeling from hyperspectral data. In the future, we will compare 3D models built from both RGB and hyperspectral images on the same project. We will also develop an effective merging technique for 3D models reconstructed with different spectral information. Other future research could be to determine new features for spectral data.

## References

[1] C. H. Bock, G. H. Poole, P. E. Parker, and T. R. Gottwald. Plant disease severity estimated visually, by digital photography and image analysis, and by hyperspectral imaging. *Critical Reviews in Plant Sciences*, 29(2):59–107, 2010.

[2] N. Brusco, S. Capeleto, M. Fedel, A. Paviotti, L. Poletto, G. Cortelazzo, and G. Tondello. A system for 3D modeling frescoed historical buildings with multispectral texture information. *Machine Vision and Applications*, 17(6):373–393, 2006.

[3] J. Canny. A computational approach to edge detection. *IEEE Transactions on Pattern Analysis and Machine Intelligence*, 8:679–698, 1986.

[4] A. Chakrabarti and T. Zickler. Statistics of real-world hyperspectral images. In *Proceedings of the IEEE Conference on Computer Vision and Pattern Recognition*, pages 193–200, 2011.

[5] C.-C. Chang and C.-J. Lin. LIBSVM: A library for support vector machines. *ACM Transactions on Intelligent Systems and Technology*, 2:27:1–27:27, 2011.

[6] Z. Fu, A. Robles-Kelly, and J. Zhou. Milis: Multiple instance learning with instance selection. *IEEE Transactions on Pattern Analysis and Machine Intelligence*, 33(5):958–977, 2006.

[7] R. T. Furbank and M. Tester. Phenomics technologies to relieve the phenotyping bottleneck. *Trends in Plant Science*, 16(12):635 – 644, 2011.

[8] L. Gu, A. Robles-Kelly, and J. Zhou. Efficient estimation of reflectance parameters from imaging spectroscopy. *IEEE Transactions on Image Processing*, 22(9):3548–3663, 2013.

[9] N. Gupta. Hyperspectral imager development at army research laboratory, 2008.

[10] S. Han, Y. Matsushita, I. Sato, T. Okabe, and Y. Sato. Camera spectral sensitivity estimation from a single image under unknown illumination by using fluorescence. In *Proceedings of the IEEE Conference on Computer Vision and Pattern Recognition*, pages 805–812, 2012.

[11] R. I. Hartley and A. Zisserman. *Multiple View Geometry in Computer Vision*. Cambridge University Press, ISBN: 0521540518, second edition, 2004.

[12] M. H. Kim, T. A. Harvey, D. S. Kittle, H. Rushmeier, J. Dorsey, R. O. Prum, and D. J. Brady. 3d imaging spec-

troscopy for measuring hyperspectral patterns on solid objects. *ACM Transactions on Graphics*, 31(4):1–11, 2012.

[13] J. Liang, J. Zhou, X. Bai, and Y. Qian. Salient object detection in hyperspectral imagery. In *Proceedings of the IEEE International Conference on Image Processing*, 2013.

[14] D. G. Lowe. Distinctive image features from scale-invariant keypoints. *International Journal of Computer Vision*, 60(2):91–110, 2004.

[15] C. Nguyen, S. Izadi, and D. Lovell. Modeling kinect sensor noise for improved 3d reconstruction and tracking. In *Proceedings of the Second Joint 3DIM/3DPVT Conference: 3D Imaging, Modeling, Processing, Visualization & Transmission*, pages 524–530, 2012.

[16] J. Nieto, S. Monteiro, and D. Viejo. 3D geological modelling using laser and hyperspectral data. In *2010 IEEE International Geoscience and Remote Sensing Symposium*, pages 4568–4571, 2010.

[17] L. Quan, P. Tan, G. Zeng, L. Yuan, J. Wang, and S. B. Kang. Image-based plant modelling, 2006.

[18] C. Wu. Towards linear-time incremental structure from motion. In *3DTV-Conference, 2013 International Conference on*, pages 127–134, 2013.

[19] C. Wu, S. Agarwal, B. Curless, and S. Seitz. Multicore bundle adjustment. In *IEEE Conference on Computer Vision and Pattern Recognition*, pages 3057–3064, 2011.

[20] Y. Zheng, S. Gu, H. Edelsbrunner, C. Tomasi, and P. Benfey. Detailed reconstruction of 3d plant root shape, 2011.